Flavor anomalies in leptoquark model with gauged $U(1)_{L_\mu - L_\tau}$

Chuan-Hung Chen[1,2,*] and Cheng-Wei Chiang[3,2,†]

[1]Department of Physics, National Cheng-Kung University, Tainan 70101, Taiwan
[2]Physics Division, National Center for Theoretical Sciences, Taipei 10617, Taiwan
[3]Department of Physics and Center for Theoretical Physics, National Taiwan University, Taipei 10617, Taiwan

(Received 5 October 2023; accepted 12 March 2024; published 5 April 2024)

In addition to anomalies associated with the muon $g-2$ and the branching ratio (BR) of $B \to D^{(*)}\tau\bar{\nu}$, Belle II recently observed an unexpectedly large BR in the $B^+ \to K^+\nu\bar{\nu}$ decay. To resolve the anomalous excesses in these observables, we propose a framework involving a leptoquark, denoted by S_1, which has the feature that down-type quarks merely couple to neutrinos but not the charged leptons, avoiding the strict constraint from the $B_s \to \mu^-\mu^+$ decay. With the introduction of the $U(1)_{L_\mu - L_\tau}$ gauge symmetry, the Z' with light mass not only resolves the muon $g-2$ anomaly, but also ensures that S_1 couples exclusively to the third-generation leptons so that only $\tau\bar{\nu}_\tau$ and τ-neutrino modes are involved in the processes $b \to c\ell\bar{\nu}$ and $b \to s\nu\bar{\nu}$, respectively. Under the dominant constraints from $|\Delta F| = 2$ processes, we find that the S_1 contributions to the BRs of $B \to K^{(*)}\nu\bar{\nu}$ and $K_L \to \pi^0\nu\bar{\nu}$ can be factorized into the same multiplicative factor multiplying the standard model predictions, and the enhancement can be up to a factor of 2. In particular, $\mathcal{B}(K^+ \to \pi^+\nu\bar{\nu})$ can reach the upper 1σ error of the experimental value, i.e., $\simeq 15.4 \times 10^{-11}$. We also show that the model can fit the new world averages of $R(D^{(*)})$ and contribute significantly to the τ polarization in the $B \to D\tau\bar{\nu}$ decay and $\mathcal{B}(B_c \to \tau\bar{\nu})$.

DOI: 10.1103/PhysRevD.109.075004

I. INTRODUCTION

Loop-induced rare processes in the standard model (SM) are commonly considered promising places for probing new physics effects. One example is the muon anomalous magnetic dipole moment (muon $g-2$), which deviates from the Dirac theory prediction through its radiative corrections and is thus sensitive to new physics contributions. Currently, using the data-driven approach to evaluate the hadronic vacuum polarization (HVP) leads to a 5.1σ deviation from the SM prediction [1,2].[1]

Using the exclusive- and hadronic-tag approaches with 362 fb^{-1} of data, the Belle II Collaboration has observed the first evidence of $B^+ \to K^+\nu\bar{\nu}$ decay, which arises from the electroweak box and penguin diagrams in the SM. The combined result from both tag approaches is reported as [12]

$$\begin{aligned}\mathcal{B}(B^+ \to K^+\nu\bar{\nu}) &= \left[2.3 \pm 0.5(\text{stat})^{+0.5}_{-0.4}(\text{syst})\right] \times 10^{-5} \\ &= (2.3 \pm 0.7) \times 10^{-5}, \end{aligned} \tag{1}$$

indicating a 2.7σ deviation from the SM prediction.

Earlier measurements by *BABAR* were reported as $(0.2 \pm 0.8) \times 10^{-5}$ [13] and $(1.5 \pm 1.3) \times 10^{-5}$ [14], while Belle's results were $(2.9 \pm 1.6) \times 10^{-5}$ [15] and $(1.0 \pm 0.6) \times 10^{-5}$ [16]. Using the weighted average, the combined branching ratio (BR) from all five data yields $\mathcal{B}(B^+ \to K^+\nu\bar{\nu}) = (1.3 \pm 0.4) \times 10^{-5}$ [12]. If we take the SM prediction to be $\mathcal{B}(B^+ \to K^+\nu\bar{\nu})^{\text{SM}} = (4.65 \pm 0.62) \times 10^{-6}$ [17], the ratio of the measurement to the SM result can be estimated as

$$R^\nu \equiv \frac{\mathcal{B}(B^+ \to K^+\nu\bar{\nu})}{\mathcal{B}(B^+ \to K^+\nu\bar{\nu})^{\text{SM}}} = 2.80 \pm 0.94. \tag{2}$$

This deviation from the SM prediction hints at the possibility of exotic interactions in $b \to s\nu\bar{\nu}$ or $b \to s +$

*physchen@mail.ncku.edu.tw
†chengwei@phys.ntu.edu.tw

[1]The first complete lattice QCD result of HVP calculated by the BMW Collaboration shows a 2.1σ deviation from the data-driven approach [3]. This results in a reduced tension between theory and experiment. Moreover, applying the recent measurement of $e^+e^- \to \pi^+\pi^-$ cross section, the CMD-3 experiment obtains a consistent result with BMW [4,5]. Nevertheless, since the CMD-3 result disagrees with earlier measurements, such as *BABAR* [6], BESIII [7], CLEO-c [8], CMD-2 [9], and KLOE [10], resolving this tension requires more lattice QCD efforts and new experiments, e.g., MUonE [11], to confirm/remove the discrepancy.

invisible processes [18–26]. In this study, we focus on the former scenario and, more generally, we investigate the rare decaying processes involving the $d_i \to d_j \nu\bar{\nu}$ transitions, where $(d_i, d_j) = (b, s)$ or (s, d).

Leptoquarks (LQs) have been broadly studied as potential solutions to the anomalies of lepton-flavor universality measured in B meson decays [27–42]. Among the scalar LQ models, the LQ S_1 with the $SU(3)_C \times SU(2)_L \times U(1)_Y$ quantum numbers $(3, 1, -2/3)$ couples down-type quarks to neutrinos but not charged leptons. Because of this distinctive feature, the effects of S_1 only affect the $d_i \to d_j \nu\bar{\nu}$ processes, but not those involving the $d_i \to d_j \ell^+\ell'^-$ transitions. The fact that current experimental measurements on $B_s \to \mu^+\mu^-$ [43,44] and $R(K^{(*)})$ [45] show no significant deviations from the SM [46] makes the S_1 model a perfect model to explain the above mentioned R^ν anomaly and to enhance the BRs of $B \to K(K^*)\nu\bar{\nu}$ in general.

In addition to enhancing the BRs of $B \to K(K^*)\nu\bar{\nu}$ decays, the S_1 model offers an explanation for the anomalies observed in $R(D^{(*)})$ [31–36]. The current experimental values are $R(D) = 0.357 \pm 0.029$ and $R(D^*) = 0.284 \pm 0.012$ [44]. The SM results obtained by various lattice QCD groups show agreement with each other [47–55], and the SM predictions averaged by the Heavy Flavor Averaging Group are given as $R(D) = 0.298 \pm 0.004$ and $R(D^*) = 0.254 \pm 0.005$ [44]. These measurements reveal an overall, notable 3.3σ deviation from the SM in the $b \to c\tau\nu$ decays [44].

The S_1 couplings to quarks and neutrinos are generally flavor dependent. It is thus a common practice in the literature to assume an arbitrary structure of the flavor couplings. However, it would be more compelling if a specific flavor structure comes from an underlying symmetry. In particular, the symmetry that may naturally suppress couplings to leptons in the first two generations holds the potential for explaining the observed excesses in $R(D^{(*)})$. Models with the $U(1)_{L_\mu - L_\tau}$ gauge symmetry, denoted by $U(1)_{\mu-\tau}$, have been extensively studied for various phenomenological reasons [56–58], including its potential role in resolving the muon $g-2$ anomaly [59–62]. It is found that if the SM is extended to include the $U(1)_{\mu-\tau}$ gauge symmetry, not only can the muon $g-2$ puzzle be resolved, we also provide a natural way to obtain desirable flavor couplings to the LQ. Additionally, due to the lepton-flavored $U(1)_{\mu-\tau}$ gauge symmetry, the LQ S_1 carrying the quantum number $F = 3B + L = 2$ can only couple to the quarks and leptons, and the diquark couplings to two quarks are suppressed [63]. Therefore, the proton still remains stable.

Once the SM symmetry is extended to include the $U(1)_{\mu-\tau}$ gauge symmetry, the model then has the following features: (i) S_1 primarily couples to the third-generation leptons, while its couplings to first- and second-generation leptons are naturally suppressed. (ii) In the absence of a new weak CP phase, there are only three independent down-type quark couplings in the model, denoted by y^q_{Lk}, that are interconnected by the Cabibbo-Kobayashi-Maskawa (CKM) matrix. This results in various flavor-changing neutral current (FCNC) processes in B and K decays involving these three parameters. (iii) The charged lepton mass matrix is forced to be diagonal due to the presence of the $U(1)_{\mu-\tau}$ gauge symmetry. Therefore, no lepton-flavor mixings are introduced if the SM Higgs doublet is the only scalar field responsible for the spontaneous electroweak symmetry breakdown. We note that the gauge coupling $g_{Z'}$ of $\mathcal{O}(10^{-4})$ with Z' mass of $\mathcal{O}(10\text{–}200)$ MeV can readily explain the muon $g-2$ anomaly, as has been studied extensively in the literature [58,60,62,64–68]. In this work, we focus on the LQ effects on the $d_i \to d_j \nu\bar{\nu}$ and $b \to c\tau\bar{\nu}_\tau$ decays.

Since the effective Hamiltonian for the $d_i \to d_j \nu\bar{\nu}$ transitions mediated by S_1 has the same interaction structure as in the SM, the BRs of $B \to K(K^*)\nu\bar{\nu}$ and $K_L \to \pi\nu\bar{\nu}$ in this model can be factorized into a scalar factor, which encodes the effects of S_1, multiplied by the SM values. When considering the stringent constraints from the $|\Delta F| = 2$ processes ($F = s$ and/or b), numerical analyses yield the typical values of y^q_{Lk} as $y^q_{L1} \sim \mathcal{O}(\lambda^2)$ and $y^q_{L2} \sim \mathcal{O}(\lambda)$ when we set $y^q_{L3} \sim \mathcal{O}(1)$, written in terms of Wolfenstein's parameter $\lambda \simeq 0.225$. With this structure of the new Yukawa couplings, the BRs for $B \to K(K^*)\nu\bar{\nu}$ and $K_L \to \pi\nu\bar{\nu}$ can possibly exceed the SM predictions by at least a factor of 2. In this case, $\mathcal{B}(K^+ \to \pi^+\nu\bar{\nu})$ can reach the upper 1σ error of the experimental value. In addition, $R(D)$ and $R(D^*)$ can be enhanced up to the central values of current data.

In the following, we will formulate the BRs for the exclusive $d_i \to d_j \nu\bar{\nu}$ processes mediated by S_1 in Sec. II. Constraints from $\Delta K = 2$ and $\Delta B_q = 2$ are analyzed in Sec. IV. Detailed numerical analysis and discussions are given in Sec. V. Our findings are summarized in Sec. VI.

II. $B \to K^{(*)}\nu\bar{\nu}$ AND $K \to \pi\nu\bar{\nu}$ VIA LQ S_1

According to the model setup, only leptons in the last two generations and S_1 carry the $U(1)_{\mu-\tau}$ charges. More explicitly, Table I shows the $SU(2)_L \times U(1)_Y \times U(1)_{\mu-\tau}$ quantum numbers of all leptons and S_1. Based on these assignments, the Yukawa interactions of the LQ S_1 are given by

TABLE I. Quantum numbers of the leptons and LQ S_1.

	$e_{L(R)}$	$\mu_{L(R)}$	$\tau_{L(R)}$	$S_1^{-\frac{1}{3}}$
$L_\mu - L_\tau$	0	1	−1	−1
$SU(2)_L$	2(1)	2(1)	2	1
$U(1)_Y$	−1(−2)	−1(−2)	1	−2/3

$$-\mathcal{L}_Y \supset \overline{Q_L^c} i\tau_2 \mathbf{y}_L^q L_\tau (S_1^{-\frac{1}{3}})^* + \overline{u_R^c} \mathbf{y}_R^u \tau_R (S_1^{-\frac{1}{3}})^* + \text{H.c.}, \quad (3)$$

where the quark-flavor indices are suppressed, $Q_L^T = (u,d)_L$ and $L_\tau^T = (\nu_\tau, \tau)_L$ represent the quark and the third-generation lepton doublets, respectively, and $F^c = C\gamma^0 F^*$ with C being the charge conjugation operator. The $U(1)_{\mu-\tau}$ gauge symmetry restricts the charged lepton mass matrix to be diagonal. Consequently, the lepton-flavor mixing matrices $V_{R,L}^\ell$ are both unit matrices, e.g., $V_{R,L}^\ell = \mathbb{1}$. This has further implications for the LQ interaction described in Eq. (3), as it only couples to the third-generation leptons due to the absence of light-charged leptons involved in the process. As a result, the interactions in Eq. (3) exclusively induce the $b \to c\tau\bar{\nu}_\tau$ decay through the Yukawa couplings y_{R2}^u and y_{L3}^q and have no contributions to the light lepton modes. In other words, $R(D^{(*)})$ can be enhanced without suppressing the additional contributions to the light lepton modes. Additionally, from the Yukawa couplings in Eq. (3), although only the τ neutrino is involved in the $d_i \to d_j \nu\bar{\nu}$ decays, we will demonstrate that the BRs for $B \to K^{(*)}\nu\bar{\nu}$ and $K \to \pi\nu\bar{\nu}$, in combination with the SM contributions, can be enhanced up to a factor of 2 compared to the SM results. Because of the lack of evidence that calls for new CP-violating sources in the processes considered in this work, CP violation originates purely from the Kobayashi-Maskawa (KM) phase in this study. Therefore, $\mathbf{y}_L^q$ and $\mathbf{y}_R^u$ are assumed to be real parameters.

Taking the up-type quarks to be the diagonalized states, Eq. (3) in terms of physical states can be expressed as

$$\begin{aligned} -\mathcal{L}_Y \supset & \left(\overline{u_L^C} \mathbf{y}_L^q P_L \tau + \overline{u_R^C} \mathbf{y}_R^u P_R \tau\right) (S^{-\frac{1}{3}})^* \\ & - \overline{d_L^C} V^T \mathbf{y}_L^q P_L \nu_\tau (S^{-\frac{1}{3}})^* + \text{H.c.}, \end{aligned} \quad (4)$$

with $V = V_L^{d\dagger}$ being the CKM matrix. We note in passing that generating neutrino mass would require additional mechanisms not explored in this work. Therefore, we will treat the neutrinos as massless particles and refrain from introducing the Pontecorvo-Maki-Nakagawa-Sakata (PMNS) matrix for describing the mixing among neutrino flavors. Even if we include the PMNS matrix in Eq. (4) when calculating the BRs for neutrino-related decays, the final results after summing up all neutrino flavors remain independent of the PMNS matrix due to its unitarity. Hence, we omit the PMNS matrix in Eq. (4).

From Eq. (4), the tree-level-induced FCNCs in the down-type quark processes are only determined by $V^T \mathbf{y}_L^q$. To reveal the flavor couplings, $\mathbf{Y}^{S_1} \equiv V^T \mathbf{y}_L^q$ can be decomposed as

$$\begin{aligned} Y_d^{S_1} &\approx V_{td} y_{L3}^q - \lambda y_{L2}^q + y_{L1}^q, \\ Y_s^{S_1} &\approx V_{ts} y_{L3}^q + y_{L2}^q + \lambda y_{L1}^q, \\ Y_b^{S_1} &\approx y_{L3}^q, \end{aligned} \quad (5)$$

where we have applied $V_{ud} \approx V_{cs} \approx V_{tb} \approx 1$, $V_{us} \approx -V_{cd} \approx \lambda$, and $V_{ts,td} \ll V_{tb}$. The ratio of $B_d - \overline{B}_d$ to $B_s - \bar{B}_s$ mixing due to purely LQ contributions is given by $\Delta m_{B_d}^{S_1} / \Delta m_{B_s}^{S_1} \sim |Y_b^{S_1*} Y_d^{S_1}|^2 / |Y_b^{S_1*} Y_s^{S_1}|^2$. To match the SM result of $\Delta m_{B_d} / \Delta m_{B_s} \sim \lambda^2$, which aligns with the experimental observations, and simultaneously achieve $R(D^{(*)})$ enhancement, the condition $|y_{L1}^q| < |y_{L2}^q| < |y_{L3}^q|$ for the Yukawa couplings is required. For processes involving the $d_i \to d_j \nu\bar{\nu}$ transitions, the only relevant new parameters are m_{S_1} and y_{Lk}^q. We will show that, when these parameters are bounded by observables of $\Delta K = 2$ and $\Delta B = 2$ processes, the model can yield significant deviations on the $B \to K^{(*)}\nu\bar{\nu}$ and $K \to \pi\nu\bar{\nu}$ processes from the SM predictions. Note that the $b \to s\tau^-\tau^+$ transition can be induced by the interactions in Eq. (4) through the box diagrams, predominantly mediated by one W and one S_1 in the loop. However, compared to the SM contribution, the box diagrams indeed are suppressed by $m_W^2 / m_{S_1}^2$. Using $Y_b^{S_1*} Y_s^{S_1} = 0.1$ and $m_{S_1} = 1.5$ TeV, the resulting Hamiltonian of the box diagrams is a factor of ∼4% smaller than that in the SM. Therefore, we neglect the S_1 contribution to $b \to s\tau^-\tau^+$.

Based on the couplings in Eq. (4), the effective interactions for $d_i \to d_j \nu\bar{\nu}$, combined with the SM contribution, are given by

$$\mathcal{H}_{\text{LQ}} = C_L^{\text{SM}} V_{td_i}^* V_{td_j} \left(X_t + C_{L,ij}^{S_1} \delta_{\ell\tau}\right) \bar{d}_i \gamma_\mu P_L d_j \bar{\nu}_\ell \gamma^\mu P_L \nu_\ell, \quad (6)$$

where $P_L = (1-\gamma_5)/2$, $X_t = 1.469 \pm 0.017$ [18], and the effective coefficients are defined as

$$C_L^{\text{SM}} = \frac{4G_F}{\sqrt{2}} \frac{\alpha_{\text{em}}}{2\pi s_W^2}, \qquad C_{L,ij}^{S_1} = -\frac{(Y_{d_i}^{S_1})^* Y_{d_j}^{S_1}}{2m_{S_1}^2 V_{td_i}^* V_{td_j} C_L^{\text{SM}}}. \quad (7)$$

Since only left-handed currents are involved in Eq. (6), the S_1 contributions to the BRs for the decays $B \to M\nu\bar{\nu}$ with $M = K$ or K^* can be factored out together with the SM result as a multiplicative factor. The resulting BRs can then be simplified as

$$\begin{aligned} \mathcal{B}(B \to M\nu\bar{\nu}) &= \mathcal{B}(B \to M\nu\bar{\nu})^{\text{SM}} R^\nu, \\ \text{with} \quad R^\nu &= \frac{2}{3} + \frac{1}{3} \left| 1 + \frac{C_{L,bs}^{S_1}}{X_t} \right|^2, \end{aligned} \quad (8)$$

where $B = B^+(B_d)$ when $M = K^+(K^{*0})$. Using the $B \to K, K^*$ form factors that combine light-cone sum-rule and lattice QCD [18,69,70] studies, the SM predictions of their BRs are [17]

$$\begin{aligned} \mathcal{B}(B^+ \to K^+ \nu\bar{\nu})^{\text{SM}} &= (4.65 \pm 0.62) \times 10^{-6}, \\ \mathcal{B}(B_d \to K^{*0} \nu\bar{\nu})^{\text{SM}} &= (10.13 \pm 0.92) \times 10^{-6}. \end{aligned} \quad (9)$$

It is worth mentioning that the current experimental upper limit for $B \to K^* \nu\bar{\nu}$ at 90% confidence level (C.L.) is $\mathcal{B}(B \to K^* \nu\bar{\nu}) < 2.7 \times 10^{-5}$ [16], where $\mathcal{B}(B \to K^* \nu\bar{\nu})$ combines the results from the charged and neutral B meson decays. Including the SM errors at 90% C.L., we obtain $R^\nu < 2.2$. We will take this upper bound as an input for the parameter scan. Since the new physics effect can be factored out, the longitudinal polarization fraction of K^* in the model is expected to be the same as that in the SM, i.e., $F_L^{\rm SM} = 0.47 \pm 0.03$ [18]. It is interesting to utilize this property to distinguish the interaction structures of potential new physics models. A formula analogous to Eq. (8) can be derived for the $B \to \pi(\rho)\nu\bar{\nu}$ decays. Utilizing the form factors obtained in Refs. [69,71], the SM predictions can be estimated as $\mathcal{B}(B^+ \to \pi^+(\rho^+)\nu\bar{\nu}) \simeq 1.8(3.7) \times 10^{-7}$. Compared to $B \to K(K^*)\nu\bar{\nu}$, these BRs are suppressed by $|V_{td}/V_{ts}|^2$. Even though their BRs could have significant deviations from the SM expectations due to the Yukawa coupling $Y_d^{S_1}$, they are still far from current experimental sensitivities, where the current upper limits are $\mathcal{B}(B^+ \to \pi^+(\rho^+)\nu\bar{\nu})^{\rm exp} < 1.4(3.9) \times 10^{-5}$ [43].

According to the interactions introduced in Eq. (6) and the parametrizations for the BRs of the $K^+ \to \pi^+\nu\bar{\nu}$ and $K_L \to \pi^0\nu\bar{\nu}$ decays as shown in Refs. [72,73], the influence of S_1 on the BRs of these decays can be obtained, respectively, as

$$\mathcal{B}(K^+ \to \pi^+\nu\bar{\nu}) = \frac{2}{3}\mathcal{B}(K^+ \to \pi^+\nu\bar{\nu})^{\rm SM} + \frac{\kappa_+(1+\Delta_{\rm EM})}{3} \times \left[\left(\frac{{\rm Im}X_{\rm eff}^{S_1}}{\lambda^5}\right)^2 + \left(\frac{{\rm Re}(V_{cs}^* V_{cd})}{\lambda} P_c(X) + \frac{{\rm Re}(X_{\rm eff}^{S_1})}{\lambda^5}\right)^2\right], \tag{10}$$

where $X_{\rm eff}^{\rm SM} = V_{ts}^* V_{td} X_t$, $X_{\rm eff}^{S_1} = X_{\rm eff}^{\rm SM} + V_{ts}^* V_{td} C_{L,sd}^{S_1}$, and $P_c(X) = 0.404 \pm 0.024$ denotes the charm-quark contribution [72–74], $\Delta_{\rm EM} = -0.003$, $\kappa_+ = (5.173 \pm 0.025) \times 10^{-11}(\lambda/0.225)^8$; and

$$\mathcal{B}(K_L \to \pi^0\nu\bar{\nu}) = \mathcal{B}(K_L \to \pi^0\nu\bar{\nu})^{\rm SM} R^\nu. \tag{11}$$

Note that it is a prediction of the model with the assumed hierarchy in the y_{Lk}^q couplings that both $\mathcal{B}(B \to M\nu\bar{\nu})$ and $\mathcal{B}(K_L \to \pi^0\nu\bar{\nu})$ have approximately the same fractional deviation, R^ν defined in Eq. (8), from their respective SM values. The SM predictions for the rare kaon decays are [17]

$$\begin{aligned}\mathcal{B}(K^+ \to \pi^+\nu\bar{\nu})^{\rm SM} &= (8.60 \pm 0.42) \times 10^{-11},\\ \mathcal{B}(K_L \to \pi^0\nu\bar{\nu})^{\rm SM} &= (2.94 \pm 0.15) \times 10^{-11}.\end{aligned} \tag{12}$$

For the $K^+ \to \pi^+\nu\bar{\nu}$ decay, the current experimental measurement, combining E949 at BNL [75] and NA62 at CERN [76], is $(11.4^{+4.0}_{-3.3}) \times 10^{-11}$. With the 2021 data analysis by KOTO, the upper limit for $K_L \to \pi^0\nu\bar{\nu}$ now is $\mathcal{B}(K_L \to \pi^0\nu\bar{\nu}) < 2 \times 10^{-9}$ [77]. From Eq. (11), it can be seen that, similar to $B \to M\nu\bar{\nu}$, the LQ contribution to $K_L \to \pi^0\nu\bar{\nu}$ can be expressed as a product of the SM prediction and a scalar factor that encodes the S_1 effects. When the small weak phase of V_{ts} is neglected, $Y_s^{S_1}$ is a real parameter, and the imaginary part of V_{td} from $Y_d^{S_1}$ for $K_L \to \pi^0\nu\bar{\nu}$ can be factored out as part of the SM prediction. Consequently, the CP-violating effect does not appear in the multiplicative factor in Eq. (11).

For $m_{Z'} \sim \mathcal{O}(100)$ MeV, $B \to K^{(*)}\nu\bar{\nu}$ can proceed through the resonant channel $B \to K^{(*)}(Z' \to)\nu\bar{\nu}$. Though the Z' gauge boson of $U(1)_{\mu-\tau}$ can only couple to the second- and third-generation leptons, by kinetic mixing with the $U(1)_Y$ gauge boson in the SM, the induced effective interactions of Z' with quarks can be written as $\mathcal{L} \supset -e\epsilon J^\mu Z'_\mu$ [78], where e is the QED coupling and J^μ is the electromagnetic current of quarks. Accordingly, the $b \to sZ'$ transition can be induced via the penguin diagram mediated by the W gauge boson and top quark, and the resulting effective Hamiltonian is obtained as

$$\begin{aligned}\mathcal{H}_{b\to sZ'} &= -C_{Z'}\bar{s}\gamma^\mu P_L b Z'_\mu\\ &= -\frac{4\sqrt{2}G_F V_{ts}^* V_{tb}}{(4\pi)^2}\left(m_t^2 Q_t e\epsilon I_0(x_t)\right)\bar{s}\gamma^\mu P_L b Z'_\mu,\end{aligned} \tag{13}$$

where $Q_t = 2/3$ is the electric charge of the top quark, $x_t = m_t^2/m_W^2$, and the loop integral is defined as

$$I_0(x_t) = \int_0^1 dy \frac{y}{1 + (x_t - 1)y}. \tag{14}$$

The effective Hamiltonian for the $b \to s\nu\bar{\nu}$ transition mediated by the light Z' can be written as

$$\mathcal{H}_{Z'} = \frac{g_{Z'} C_{Z'}}{q^2 - m_{Z'}^2 + i m_{Z'}\Gamma_{Z'}}\bar{s}\gamma_\mu P_L b \bar{\nu}_{\ell'}\gamma^\mu P_L \nu_{\ell'}, \tag{15}$$

where $\ell' = \mu, \tau, \Gamma_{Z'}$ is the width of the Z' gauge boson, and q^2 is the invariant mass of the neutrino pair. The total effective Hamiltonian for the $b \to s\nu\bar{\nu}$ transition should combine Eqs. (15) and (6). However, because the Z'-mediated contribution becomes dominant at the Z' resonance, i.e., when $q^2 \approx m_{Z'}^2$, the BRs of $B \to K^{(*)}\nu\bar{\nu}$ can be decomposed as $\mathcal{B}(B \to K^{(*)}\nu\bar{\nu}) = \mathcal{B}(B \to K^{(*)}\nu\bar{\nu})^{\rm LQ} + \mathcal{B}(B \to K^{(*)}Z') \times \mathcal{B}(Z' \to \nu\bar{\nu})$. The BRs for $B \to (K, K^*)Z'$ can be obtained as

$$\mathcal{B}(B^+ \to K^+ Z') = \tau_{B^+}\frac{m_B |C_{Z'} f_+(m_{Z'}^2)|^2}{64\pi}\frac{m_B^2}{m_{Z'}^2}, \tag{16}$$

$$\mathcal{B}(B_d \to K^{*0} Z') = \tau_{B_d} \frac{m_B |C_{Z'} A_{12}(m_{Z'}^2)|^2}{\pi} \frac{m_{K^{*0}}^2}{m_{Z'}^2}, \quad (17)$$

where τ_{B^+} and τ_{B_d} are the lifetimes of B^+ and B_d, respectively, and $f_+(q^2)$ and $A_{12}(q^2)$ are the $B \to (K, K^*)$ form factors. We note that the longitudinal components of K^* and Z' in $B_d \to K^{*0} Z'$ play the dominant effect, where the associated form factors $A_{1,2}(q^2)$ are derived from the axial vector current. Because of the fact that $m_{K^{*0}} \ll m_{B_d}$, the related form factors in the BR can be simplified as $A_1(q^2) - A_2(q^2) \approx 16 A_{12}(q^2) m_{K^{*0}}^2 / m_{B_d}^2$ [69]. Taking $m_{Z'} = 100$ MeV, $\epsilon = 9.4 \times 10^{-6}$, $f_+(m_{Z'}^2) = 0.31$ [79], and $A_{12}(m_{Z'}^2) = 0.256$ [69], we obtain $\mathcal{B}(B^+ \to K^+ Z') \simeq 3.35 \times 10^{-7}$ and $\mathcal{B}(B_d \to K^{*0} Z') \simeq 3.90 \times 10^{-7}$, while the muon $g-2$ correction in this case is estimated to be $\Delta a_\mu \sim 1.0 \times 10^{-9}$. Even with $\mathcal{B}(Z' \to \nu\bar{\nu}) = 1$, the BRs for the $B \to K^{(*)} \nu\bar{\nu}$ decays from the resonant Z' contribution are at least 1 order of magnitude smaller than the SM predictions. Therefore, the Z' effect on $B \to K^{(*)} \nu\bar{\nu}$ can be neglected. The same conclusion can be applied to the $K \to \pi\nu\bar{\nu}$ decays.

III. OBSERVABLES IN $B \to D^{(*)} \tau\bar{\nu}$ AND $B_c \to \tau\bar{\nu}$

The Yukawa couplings $y_{L3,L2}^q$, together with y_{R2}^u, contribute to the $b \to c\tau\bar{\nu}_\tau$ transition. To illustrate the influence on the observables related to the exclusive $b \to c\tau\bar{\nu}_\tau$ decays in the model, we show the effective Hamiltonian for $b \to c\ell\bar{\nu}$ mediated by W and $S_1^{-1/3}$ as [62]

$$\mathcal{H}_{b\to c\ell\nu} = \frac{4 G_F V_{cb}}{\sqrt{2}} \big[(1 + C_V^\ell \delta_\tau^\ell) \bar{c} \gamma^\mu P_L b \bar{\ell} \gamma_\mu P_L \nu_\ell + C_S^\tau \bar{c} P_L b \bar{\tau} P_L \nu_\tau + C_T^\tau \bar{c} \sigma_{\mu\nu} P_L b \bar{\tau} \sigma^{\mu\nu} P_L \nu_\tau \big], \quad (18)$$

where the effective Wilson coefficients at the m_{S_1} scale are given by

$$C_V^\tau = \frac{\sqrt{2}}{4 G_F V_{cb}} \frac{y_{L3}^q y_{L2}^q}{2 m_{S_1}^2}, \qquad C_S^\tau = -\frac{\sqrt{2}}{4 G_F V_{cb}} \frac{y_{L3}^q y_{R2}^u}{2 m_{S_1}^2},$$
$$C_T^\tau = \frac{\sqrt{2}}{4 G_F V_{cb}} \frac{y_{L3}^q y_{R2}^u}{8 m_{S_1}^2}. \quad (19)$$

The effective couplings C_S^τ and C_T^τ at the m_b scale can be obtained from the LQ mass scale via the renormalization group equations. Following the results in Ref. [80], we obtain $C_S^\tau(m_b) \approx 1.57 C_S^\tau$ and $C_T^\tau(m_b) \approx 0.86 C_T^\tau$. It can be seen that, although C_V^τ, which has the same current-current interaction structure as the SM, can be induced, due to the fact that $|y_{L2}^q| < |y_{L3}^q|$, the dominant effects by S_1 are through the scalar and tensor operators.

Some interesting observables related to the $b \to c\tau\bar{\nu}_\tau$ transition include $R(D^{(*)})$, defined as the ratios of $\mathcal{B}(B \to D^{(*)} \tau\bar{\nu}_\tau)$ to $\mathcal{B}(B \to D^{(*)} \ell\bar{\nu}_\ell)$ with ℓ being the light leptons; $P_\tau(D^{(*)})$, the τ polarization in the $B \to D^{(*)} \tau\bar{\nu}_\tau$ decays; the longitudinal polarization $F_L^{D^*}$ of D^* in the $B \to D^* \tau\bar{\nu}_\tau$ decay; and $\mathcal{B}(B_c \to \tau\bar{\nu}_\tau)$. For numerical analyses, we employ the simplified results [81]

$$\frac{R(D)}{R(D)^{\rm SM}} \approx |1 + C_V^\tau|^2 + |C_S^\tau|^2 + 0.9 |C_T^\tau|^2 + {\rm Re}\big[1.49 C_S^\tau + 1.14 C_T^\tau\big], \quad (20a)$$

$$\frac{R(D^*)}{R(D^*)^{\rm SM}} \approx |1 + C_V^\tau|^2 + 16.07 |C_T^\tau|^2 + {\rm Re}\big[-0.11 C_S^\tau - 5.12 C_T^\tau\big], \quad (20b)$$

$$\frac{P_\tau^D}{P_\tau^{D,{\rm SM}}} \approx \left(\frac{R(D)}{R(D)^{\rm SM}}\right)^{-1} \Big(|1 + C_V^\tau|^2 + 3.18 |C_S^\tau|^2 + 0.18 |C_T^\tau|^2 + {\rm Re}\big[4.65 C_S^\tau - 1.18 C_T^\tau\big] \Big), \quad (20c)$$

$$\frac{P_\tau^{D^*}}{P_\tau^{D^*,{\rm SM}}} \approx \left(\frac{R(D^*)}{R(D^*)^{\rm SM}}\right)^{-1} \Big(|1 + C_V^\tau|^2 - 0.07 |C_S^\tau|^2 - 1.86 |C_T^\tau|^2 + {\rm Re}\big[0.22 C_S^\tau - 3.37 C_T^\tau\big] \Big), \quad (20d)$$

$$\frac{F_L^{D^*}}{F_L^{D^*,{\rm SM}}} \approx \left(\frac{R(D^*)}{R(D^*)^{\rm SM}}\right)^{-1} \Big(|1 + C_V^\tau|^2 + 0.08 |C_S^\tau|^2 + 7.02 |C_T^\tau|^2 + {\rm Re}\big[-0.24 C_S^\tau - 4.37 C_T^\tau\big] \Big). \quad (20e)$$

The SM results are obtained as $P_\tau^{D,{\rm SM}} = 0.325 \pm 0.009$, $P_\tau^{D^*,{\rm SM}} = -0.497 \pm 0.013$, and $F_L^{D^*,{\rm SM}} = 0.46 \pm 0.04$ [81], whereas the current experimental measurements are $P_\tau^{D^*,{\rm exp}} = -0.38 \pm 0.51^{+0.21}_{-0.16}$ [82] and $F_L^{D^*,{\rm exp}} = 0.491 \pm 0.053$ [83,84]. The value of $F_L^{D^*,{\rm exp}}$ is estimated by weighted averaging the measurements of Belle and LHCb. On the other hand, the BR of $B_c \to \tau\bar{\nu}_\tau$ can be expressed as

$$\mathcal{B}(B_c \to \tau\bar{\nu}_\tau) = \mathcal{B}(B_c \to \tau\bar{\nu}_\tau)^{\rm SM} \times \left| 1 + C_V^\tau - \frac{m_{B_c}^2}{(m_b + m_c) m_\tau} C_S^\tau \right|^2, \quad (21)$$

with $\mathcal{B}(B_c \to \tau\bar{\nu}_\tau)^{\rm SM} \simeq 2.0\%$ [85].

IV. CONSTRAINTS FROM $\Delta K = 2$ AND $\Delta B = 2$

Since the down-type quarks only couple to the left-handed neutrinos via the LQ S_1, strict constraints on the parameters y_{Lk}^q come from the $|\Delta F| = 2$ processes that are

induced via the box diagrams, where ν_τ and S_1 run in the box loops. Thus, the effective Hamiltonian for $|\Delta F| = 2$ can be derived in a straightforward way as

$$\mathcal{H}(|\Delta F| = 2) \approx \frac{1}{8}\frac{(Y_{d_i}^{S_1*} Y_{d_j}^{S_1})^2}{(4\pi)^2 m_{S_1}^2}(\bar{d}_i \gamma_\mu P_L d_j)^2. \tag{22}$$

Using the matrix element $\langle F|(\bar{q}'\gamma_\mu P_L q)^2|F\rangle = f_F^2 B_F m_F/3$, $\Delta m_K = 2\mathrm{Re}(M_{12}^K)$ and $\Delta m_{B_q} = 2|M_{12}^B|$, the mass differences for K-$\bar{K}$ and $B_q - \bar{B}_q$ mixings can be formulated as

$$\Delta m_K^{S_1} = \frac{\mathrm{Re}(Y_s^{S_1*} Y_d^{S_1})^2}{64\pi^2 m_{S_1}^2}\frac{f_K^2 B_K m_K}{3},$$
$$\Delta m_{B_q}^{S_1} = \frac{|Y_b^{S_1*} Y_q^{S_1}|^2}{64\pi^2 m_{S_1}^2}\frac{f_{B_q}^2 B_{B_q} m_{B_q}}{3}, \tag{23}$$

where f_F is the decay constant of the F meson and B_F is the bag parameter. Since the SM predictions on Δm_K and Δm_{B_q} are consistent with experimental data and the uncertainties from theoretical nonperturbative QCD effects are larger than those of data, to bound the parameters y_{Lk}^q we conservatively require that the new physics contribution is at least 1 order of magnitude smaller than the central value of data; that is, we assume

$$\Delta m_{K,B_q}^{S_1} \lesssim 0.1 \Delta m_{K,B_q}^{\mathrm{exp}}, \tag{24}$$

where the current data are $\Delta m_K^{\mathrm{exp}} = (5.293 \pm 0.009)\ (\mathrm{ns})^{-1}$, $\Delta m_{B_d}^{\mathrm{exp}} = 0.5065 \pm 0.0019\ (\mathrm{ps})^{-1}$, and $\Delta m_{B_s}^{\mathrm{exp}} = (17.765 \pm 0.006)\ (\mathrm{ps})^{-1}$ [43].

To illustrate the $|\Delta F| = 2$ constraints, we show the contours of the mass differences with respect to y_{Lk}^q in Fig. 1, where $y_{L3}^q = 0.8$ and $y_{L1}^q = 0.02$ are used for Δm_K (left plot) and Δm_{B_q} (right plot), respectively. For numerical estimates, we have set $m_{S_1} = 1.5$ TeV, $f_K\sqrt{B_K} = 0.132$ GeV, $f_{B_d}\sqrt{B_d} = 0.174$ GeV, $f_{B_s}\sqrt{B_s} = 0.21$ GeV [86], $\lambda = 0.223$, $V_{td} = A\lambda^2(1-\rho-i\eta)$ with $A = 0.833$, $\rho = 0.163$, and $\eta = 0.357$, and $V_{ts} = -0.041$ [43]. From the plots, it is seen that $|y_{L1}^q| < |y_{L2}^q| < |y_{L3}^q|$ is preferred when $|y_{L3}^q| \sim \mathcal{O}(1)$, as required to explain $R(D^{(*)})$. We note that the results for $y_{L3}^q = -0.8$ and $y_{L1}^q = -0.02$ can be obtained from the corresponding plots in Fig. 1 by making a parity transformation on the parameters, i.e., $y_{L1,L2}^q \to -y_{L1,L2}^q$ for Δm_K and $y_{L2,L3}^q \to -y_{L2,L3}^q$ for Δm_{B_q}. We also note in passing that the parameter distributions for Δm_K and Δm_{B_d} do not center at the origin in the respective plots because of our choices of $y_{L3}^q = 0.8$ and $y_{L1}^q = 0.02$. The distribution for Δm_{B_s} in Fig. 1(b), on the other hand, is symmetric with respect to the origin because it is insensitive to the choice of y_{L1}^q.

V. NUMERICAL RESULTS AND DISCUSSIONS

In this section, we analyze the S_1 contributions to the $B \to M\nu\bar{\nu}$ and $K \to \pi\nu\bar{\nu}$ decays when the constraints from $|\Delta F| = 2$ are all taken into account. In this model, the LQ only couples to the third-generation lepton, and the involved parameters in the model are y_{Lk}^q and m_{S_1}. Both CMS [87] and ATLAS [88] have searched for the scalar LQ with a charge of $e/3$ using the $t\tau$ and $b\nu$ production channels. An upper bound on the LQ mass is given by ATLAS to be $m_S \geq 1.22$ TeV when $\mathcal{B}(S_1 \to t\tau) = 1/2$.

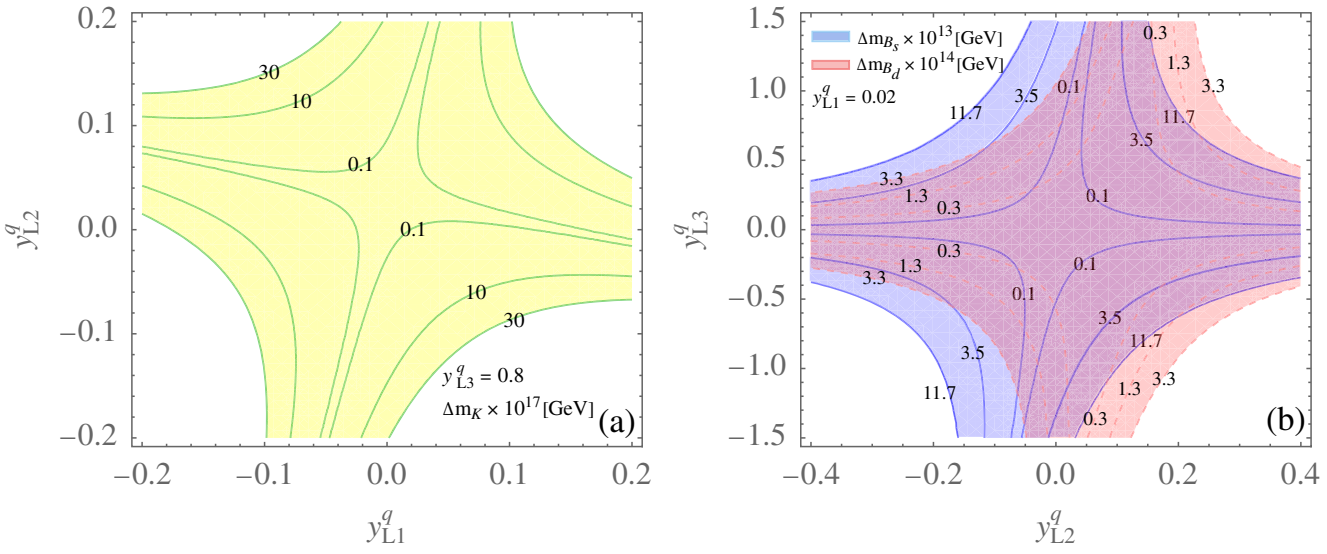

FIG. 1. (a) $\Delta m_K^{S_1}$ (in units of GeV) with $y_{L3}^q = 0.8$ as a function of y_{L1}^q and y_{L2}^q. (b) $\Delta m_{B_q}^{S_1}$ (in units of GeV) with $y_{L1}^q = 0.02$. In both plots, $\Delta m_{K,B_q}^{S_1} \lesssim 0.1\Delta m_{K,B_q}^{\mathrm{exp}}$ is applied.

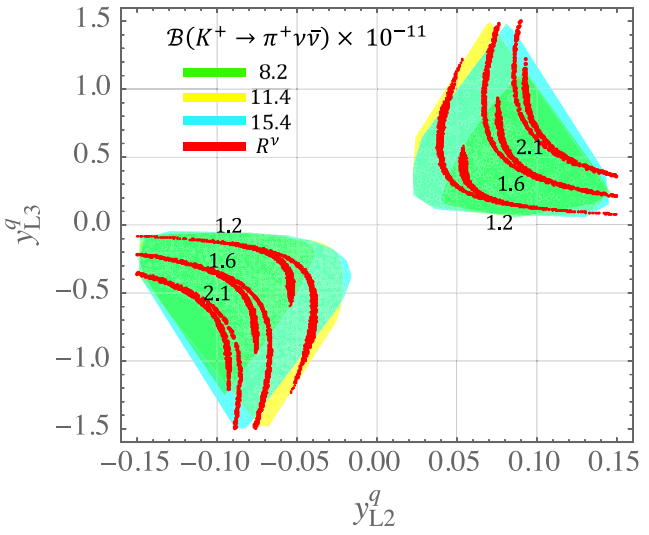

FIG. 2. Predictions for $\mathcal{B}(K^+ \to \pi^+ \nu\bar{\nu})$ and R^ν in the plane of y^q_{L2} and y^q_{L3}, with y^q_{L1} varying within the specified range and under the constraints discussed in the main text.

Given this measurement and the allowed parameter ranges in Fig. 1, $t\tau$ and $b\nu_\tau$ are the dominant decays of the LQ in the model. Thus, we take $m_{S_1} = 1.5$ TeV in our numerical calculations. Since $|y^q_{L3}|$ as large as 1.5 for $m_{S_1} = 1.5$ TeV is still not excluded by the current data, we therefore consider $|y^q_{L3}| \lesssim 1.5$ in the following analysis. Using the high-p_T tail of the $pp \to \tau\tau$ distribution measured by ATLAS [89] with the integrated luminosity of 139 fb^{-1}, the bound on the $c - \tau - S_1$ coupling can be obtained as $|y^u_{R2}| \lesssim 1.6$ [90]. The consistent result using the Drell-Yan high-p_T tail can be found in Refs. [91,92].

To conduct a numerical analysis of the $d_i \to d_j \nu\bar{\nu}$ transitions, we need to identify suitable ranges for the parameters y^q_{Lk}. Guided by the observation that $\Delta m^{\rm exp}_{B_d}/\Delta m^{\rm exp}_{B_s} \sim \lambda^2$, we consider $|Y^{S_1}_d/Y^{S_1}_s| \sim \mathcal{O}(\lambda)$ for the LQ contributions to align with the experimental constraints. From Eq. (5), as we assume $|y^q_{L3}| \sim \mathcal{O}(1)$, the appropriate values for $y^q_{L1,L2}$ should be chosen as $|y^q_{L1}| \sim \mathcal{O}(\lambda^2)$ and $|y^q_{L2}| \sim \mathcal{O}(\lambda)$. Thus, to determine the parameter space of the three parameters y^q_{Lk} under the constraints of $|\Delta F| = 2$ processes, we perform a random parameter scan within the following ranges:

$$y^q_{L1} \in (-0.05, 0.05), \qquad y^q_{L2} \in (-0.15, 0.15),$$
$$y^q_{L3} \in (-1.5, 1.5). \tag{25}$$

The ranges of $\Delta m^{S_1}_{K,B_q}$ that satisfy the conditions in Eq. (24) are explicitly taken as follows: $\Delta m^{S_1}_K \in (0.01, 34.8) \times 10^{-17}$ GeV, $\Delta m^{S_1}_{B_d} \in (0.01, 33.3) \times 10^{-15}$ GeV, and $\Delta m^{S_1}_{B_s} \in (0.01, 11.7) \times 10^{-13}$ GeV. According to the current experimental upper limit of $B \to K^* \nu\bar{\nu}$, we require $R^\nu < 2.2$ in the parameter scan. Additionally, we will require that the predicted $\mathcal{B}(K^+ \to \pi^+ \nu\bar{\nu})$ fall within its $\pm 1\sigma$ range.

Using 10^7 sampling points and the constraints mentioned above, the predicted BR for $K^+ \to \pi^+ \nu\bar{\nu}$ in the y^q_{L2}-y^q_{L3} plane is shown in Fig. 2, where the green, yellow, and cyan regions give the BRs of $(8.2, 11.4, 15.4) \times 10^{-11}$, respectively. The reason for such a spreading pattern for each specific BR is because of the more intricate dependence of y^q_{Lk} in $\mathcal{B}(K^+ \to \pi^+ \nu\bar{\nu})$, as revealed in Eq. (11), than that in $\mathcal{B}(B \to M\nu\bar{\nu})$ and $\mathcal{B}(K_L \to \pi^0 \nu\bar{\nu})$. It is also because of this observable that, compared to considering only $\Delta m_{K,B_d,B_s}$ as the examples in Fig. 1, the preferred parameter space in the plane is restricted to the first and third quadrants. Note that the parameter space around the origin is excluded because

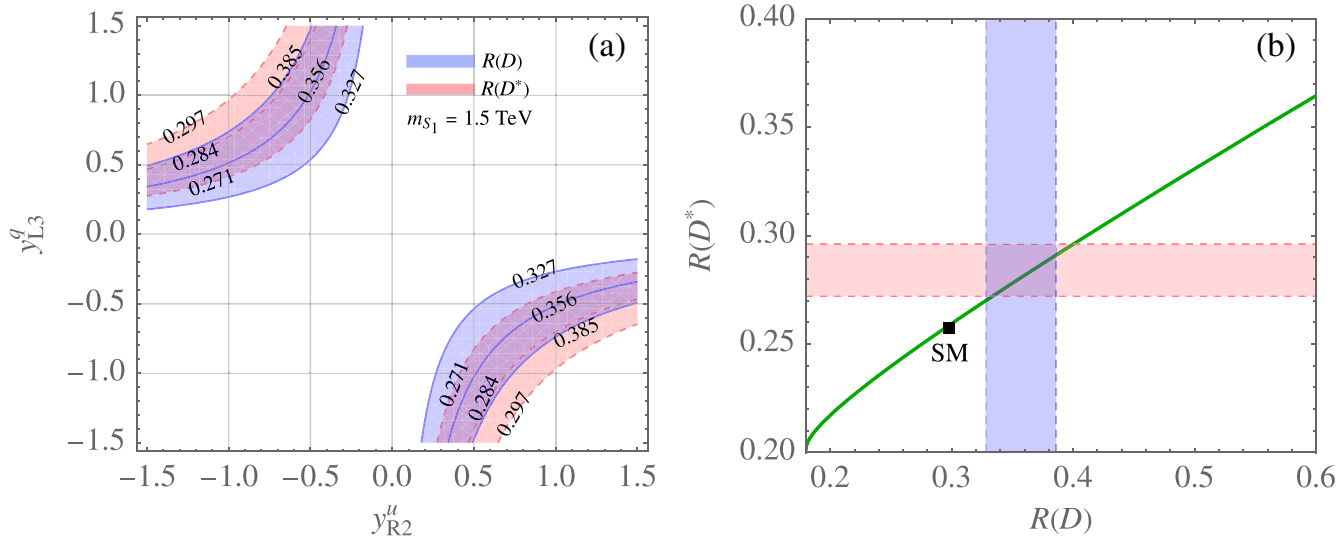

FIG. 3. (a) Contours of $R(D^{(*)})$ in the y^u_{R2}-y^q_{L3} plane and (b) correlation between $R(D)$ and $R(D^*)$ in the model. The light blue and pink bands represent the $\pm 1\sigma$ bands of $R(D)$ and $R(D^*)$, respectively. The solid square marks the SM predictions.

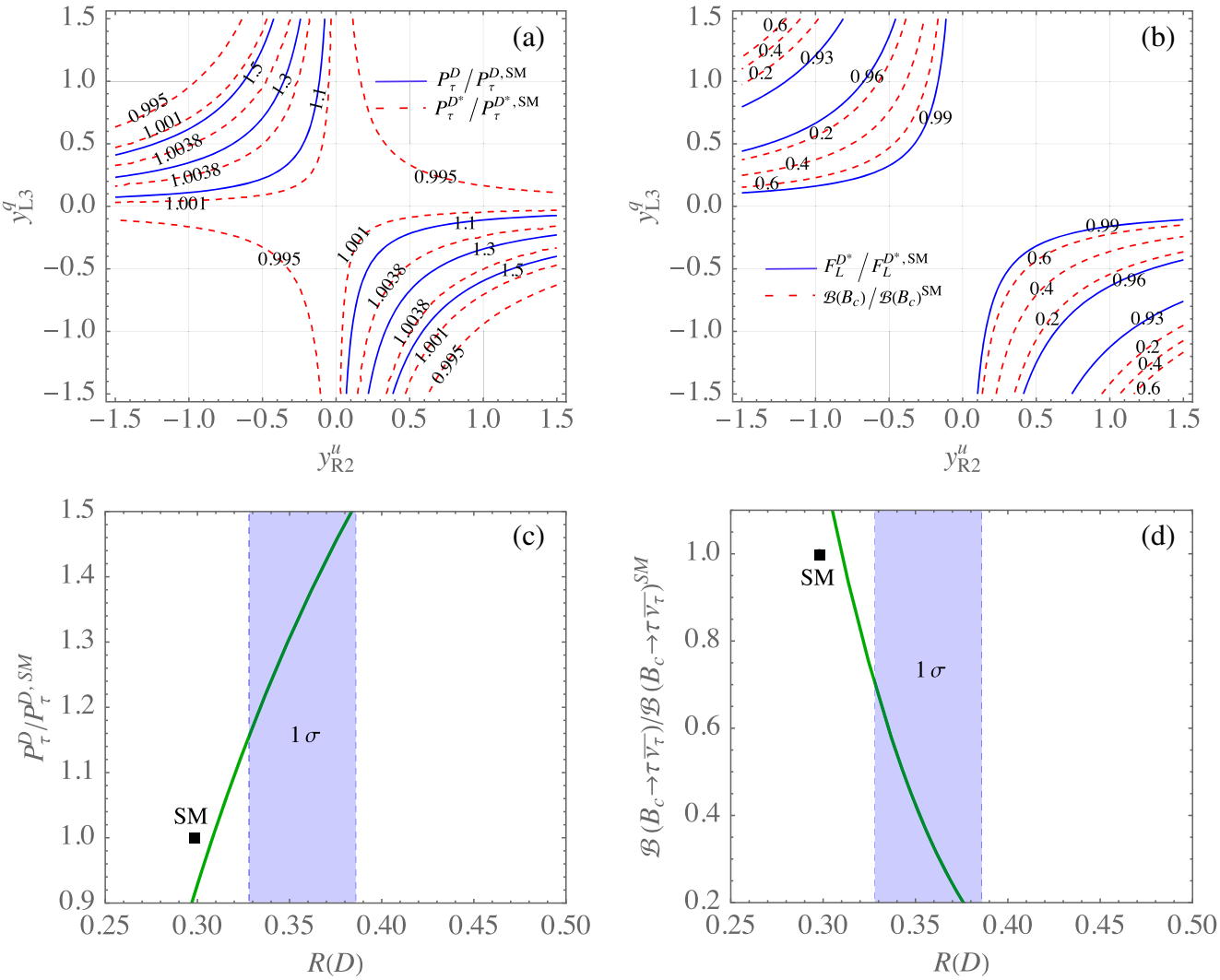

FIG. 4. (a) Contours of $P^D_\tau/P^{D,\mathrm{SM}}_\tau$ (blue solid) and $P^{D^*}_\tau/P^{D^*,\mathrm{SM}}_\tau$ (red dashed) in the y^u_{R2}-y^q_{L3} plane. (b) Contours of $F^{D^*}_L/F^{D^*,\mathrm{SM}}_L$ (solid) and $\mathcal{B}(B_c)/\mathcal{B}(B_c)^{\mathrm{SM}}$ (dashed) in the y^u_{R2}-y^q_{L3} plane, where $\mathcal{B}(B_c)\equiv\mathcal{B}(B_c\to\tau\bar{\nu}_\tau)$. The green solid curves in (c) and (d) show the correlations of $P^D_\tau/P^{D,\mathrm{SM}}_\tau$ and $\mathcal{B}(B_c\to\tau\bar{\nu}_\tau)/\mathcal{B}(B_c\to\tau\bar{\nu}_\tau)^{\mathrm{SM}}$ with $R(D)$, respectively. The shaded areas correspond to the $\pm1\sigma$ region of the observed $R(D)$ and the solid squares are the SM predictions.

we have assumed minimum new physics contributions to $\Delta m^{S_1}_{K,B_d,B_s}$. This is also required in order to have significant deviations in $\mathcal{B}(B\to M\nu\bar{\nu})$ and $\mathcal{B}(K_L\to\pi^0\nu\bar{\nu})$.

As alluded to before, the S_1 contributions to $\mathcal{B}(B\to M\nu\bar{\nu})$ and $\mathcal{B}(K_L\to\pi^0\nu\bar{\nu})$ can be factored out together with the SM contributions into a scalar factor characterized by R^ν defined in Eq. (8). We superimpose the distribution for $R^\nu=(1.2, 1.8, 2.6)$ in Fig. 2 to show that such values are consistent with the current measurement of $\mathcal{B}(K^+\to\pi^+\nu\bar{\nu})$. The dispersion in each particular value of R^ν is due to the variation in y^q_{L1}. This means that the BRs of $\mathcal{B}(B\to M\nu\bar{\nu})$ and $\mathcal{B}(K_L\to\pi^0\nu\bar{\nu})$ are allowed to be enhanced by a factor of 2 or more, thus accommodating the Belle II data in Eq. (2).

Finally, we show the impact of S_1 on the observables in the exclusive $b\to c\tau\bar{\nu}$ decay. Neglecting the minor influence of C^τ_V in Eq. (19), the parameters involved in the $b\to c\tau\nu$ transition appear in the combination $y^q_{L3}y^u_{R2}/m^2_{S_1}$. Using the formulas given in Eqs. (20a) and (20b), we show in Fig. 3(a) several contours of $R(D)$ and $R(D^*)$ in the plane of y^u_{R2} and y^q_{L3} for the case of $m_{S_1}=1.5$ TeV. The $\pm1\sigma$ ranges of $R(D)$ and $R(D^*)$ data are seen to have a significant overlap. The correlation between $R(D)$ and $R(D^*)$ as we vary the value of the dominant factor $y^q_{L3}y^u_{R2}$ is shown in Fig. 3(b), where the SM predictions $R^{\mathrm{SM}}(D)\approx0.298$ and $R^{\mathrm{SM}}(D^*)\approx0.254$ are marked by the black square. Because of the absence of a significant interfering effect between the SM and S_1 contributions, the linear relationship between $R(D)$ and $R(D^*)$ does not depend on the values of the parameters involved (e.g., m_{S_1}). The fact that the predicted correlation curve goes through a good portion of the crossed region reflects the overlapped parameter space in Fig. 3(a). A more precise determination

of both $R(D)$ and $R(D^*)$ will be able to show whether they are still in line with the model predictions.

Based on Eqs. (20c) and (20d), we plot contours for the ratios of P_τ^D and $P_\tau^{D^*}$ to their respective SM values in the y_{R2}^u-y_{L3}^q plane in Fig. 4(a), where the solid curves represent $P_\tau^D/P_\tau^{D,\mathrm{SM}}$ and the dashed curves are for $P_\tau^{D^*}/P_\tau^{D^*,\mathrm{SM}}$. Compared to P_τ^{D*}, P_τ^D exhibits more sensitivity to the effects of S_1. This behavior can be simply understood as follows: The terms of linear C_S^τ and C_T^τ dominate the contributions to the τ-lepton polarization. Since the coefficient of C_S^τ is much larger in P_τ^D than in $P_\tau^{D^*}$ and $C_T^\tau/C_S^\tau = 1/4$, P_τ^D receives a more significant influence from the LQ S_1. We note that $y_{L3}^q y_{R2}^u < 0$ due to the $R(D^{(*)})$ excesses; therefore, P_τ^D is enhanced by the mediation of S_1. Using Eqs. (20e) and (21), we show contours denoting the ratios of $F_L^{D^*}$ (solid) and $\mathcal{B}(B_c \to \tau\bar{\nu}_\tau)$ (dashed) to their respective SM values in Fig. 4(b). From Eq. (20e), the contributions from linear C_S^τ and C_T^τ in $F_L^{D^*}$ have a comparable dependence to those in $P_\tau^{D^*}$. Thus, $F_L^{D^*}$ is not significantly affected by the LQ S_1. Moreover, according to Eq. (21), the enhancement factor $m_{B_c}^2/((m_b + m_c)m_\tau)$ due to the LQ contribution leads to a considerable reduction in $\mathcal{B}(B_c \to \tau\bar{\nu}_\tau)$.

To illustrate the fact that the observables $R(D)$, P_τ^D, and $\mathcal{B}(B_c \to \tau\bar{\nu}_\tau)$ are more sensitive to the LQ effects, we show the correlations of $P_\tau^D/P_\tau^{D,\mathrm{SM}}$ and $\mathcal{B}(B_c \to \tau\bar{\nu}_\tau)/\mathcal{B}(B_c \to \tau\bar{\nu}_\tau)^{\mathrm{SM}}$ with $R(D)$ in Figs. 4(c) and 4(d), respectively, where the solid squares denote the SM predictions and the shaded areas are the current experimental data for $R(D)$ within 1σ errors. Currently, P_τ^D and $\mathcal{B}(B_c \to \tau\bar{\nu}_\tau)$ have not been observed in experiment yet. Nevertheless, their future measurements can further test whether the S_1 effects can serve as a viable explanation for the anomalies observed in $R(D)$ and $R(D^*)$.

VI. SUMMARY

Motivated by the surprisingly large branching ratio of $B^+ \to K^+\nu\bar{\nu}$ reported by the Belle II Collaboration, we have constructed a model that not only enhances $\mathcal{B}(B^+ \to K^+\nu\bar{\nu})$ but also provides an explanation for the muon $g-2$ and $\mathcal{B}(B \to D^{(*)}\tau\bar{\nu})$, where the long-standing inconsistencies between the SM predictions and the experimental measurements have not yet resolved. It is found that the leptoquark S_1 with a light Z' gauge boson under the assumed $U(1)_{L_\mu - L_\tau}$ gauge symmetry can provide the required mechanism to enhance these observables.

In addition to resolving the muon $g-2$ anomaly through the loop mediation of a light Z', the introduced $U(1)_{L_\mu - L_\tau}$ symmetry ensures that S_1 only couples to the third-generation leptons. Therefore, the S_1 LQ only contributes to the $b \to c\tau\bar{\nu}_\tau$ transition and does not affect the light lepton modes. As a result, the predicted $R(D)$ and $R(D^*)$ values can explain the excesses observed in the experimental data.

Because of the characteristic couplings of S_1, the induced $d_i \to d_j\nu\bar{\nu}$ processes involve solely the τ neutrino and depend only on the three Yukawa couplings y_{Lk}^q. When considering constraints from Δm_K and $\Delta m_{B_{d,B_s}}$, the $B \to K(K^*)\nu\bar{\nu}$, $K^+ \to \pi^+\nu\bar{\nu}$, and $K_L \to \pi^0\nu\bar{\nu}$ processes can be significantly enhanced by the effects of S_1. Such enhancements can be readily tested in future experiments. We emphasize that the KM phase is assumed to be the sole source of CP violation in the study; nevertheless, the CP-violating process $K_L \to \pi^0\nu\bar{\nu}$ can still be enhanced up to a factor of 2 compared to the SM prediction.

In addition to the impact on $R(D)$ and $R(D^*)$, we also discuss the S_1 contributions to the τ polarizations in $B \to (D, D^*)\tau\bar{\nu}_\tau$, the longitudinal polarization of D^* in $B \to D^*\tau\bar{\nu}_\tau$, and the branching ratio of $B_c \to \tau\bar{\nu}_\tau$. We have found that the τ-lepton polarization in $B \to D\tau\bar{\nu}_\tau$ and the branching ratio of $B_c \to \tau\bar{\nu}_\nu$ are more sensitive to the S_1 effects, where the former is enhanced over the SM prediction, while the latter is significantly reduced due to the LQ contribution.

ACKNOWLEDGMENTS

This work was supported in part by the National Science and Technology Council, Taiwan under Grants No. MOST-110-2112-M-006-010-MY2 (C.-H. C.) and No. MOST-111-2112-M-002-018-MY3 (C.-W. C.).

[1] D. P. Aguillard *et al.* (Muon $g-2$ Collaboration), Phys. Rev. Lett. **131**, 161802 (2023).
[2] T. Aoyama, N. Asmussen, M. Benayoun, J. Bijnens, T. Blum, M. Bruno, I. Caprini, C. M. Carloni Calame, M. Cè, G. Colangelo *et al.*, Phys. Rep. **887**, 1 (2020).
[3] S. Borsanyi *et al.*, Nature (London) **593**, 51 (2021).
[4] F. V. Ignatov *et al.* (CMD-3 Collaboration), arXiv:2302.08834.
[5] F. V. Ignatov *et al.* (CMD-3 Collaboration), arXiv:2309.12910.
[6] J. P. Lees *et al.* (*BABAR* Collaboration), Phys. Rev. D **86**, 032013 (2012).

[7] M. Ablikim *et al.* (BESIII Collaboration), Phys. Lett. B **753**, 629 (2016); **812**, 135982(E) (2021).
[8] T. Xiao, S. Dobbs, A. Tomaradze, K. K. Seth, and G. Bonvicini, Phys. Rev. D **97**, 032012 (2018).
[9] R. R. Akhmetshin *et al.* (CMD-2 Collaboration), Phys. Lett. B **648**, 28 (2007).
[10] A. Anastasi *et al.* (KLOE-2 Collaboration), J. High Energy Phys. 03 (2018) 173.
[11] P. Banerjee, C. M. Carloni Calame, M. Chiesa, S. Di Vita, T. Engel, M. Fael, S. Laporta, P. Mastrolia, G. Montagna, O. Nicrosini *et al.*, Eur. Phys. J. C **80**, 591 (2020).
[12] I. Adachi *et al.* (Belle-II Collaboration), arXiv:2311.14647.
[13] P. del Amo Sanchez *et al.* (*BABAR* Collaboration), Phys. Rev. D **82**, 112002 (2010).
[14] J. P. Lees *et al.* (*BABAR* Collaboration), Phys. Rev. D **87**, 112005 (2013).
[15] O. Lutz *et al.* (Belle Collaboration), Phys. Rev. D **87**, 111103 (2013).
[16] J. Grygier *et al.* (Belle Collaboration), Phys. Rev. D **96**, 091101 (2017).
[17] A. J. Buras and E. Venturini, Eur. Phys. J. C **82**, 615 (2022).
[18] A. J. Buras, J. Girrbach-Noe, C. Niehoff, and D. M. Straub, J. High Energy Phys. 02 (2015) 184.
[19] T. E. Browder, N. G. Deshpande, R. Mandal, and R. Sinha, Phys. Rev. D **104**, 053007 (2021).
[20] P. Asadi, A. Bhattacharya, K. Fraser, S. Homiller, and A. Parikh, J. High Energy Phys. 10 (2023) 069.
[21] P. Athron, R. Martinez, and C. Sierra, J. High Energy Phys. 02 (2024) 121.
[22] R. Bause, H. Gisbert, and G. Hiller, Phys. Rev. D **109**, 015006 (2024).
[23] L. Allwicher, D. Becirevic, G. Piazza, S. Rosauro-Alcaraz, and O. Sumensari, Phys. Lett. B **848**, 138411 (2024).
[24] T. Felkl, A. Giri, R. Mohanta, and M. A. Schmidt, Eur. Phys. J. C **83**, 1135 (2023).
[25] H. K. Dreiner, J. Y. Günther, and Z. S. Wang, arXiv:2309.03727.
[26] Y. Amhis, M. Kenzie, M. Reboud, and A. R. Wiederhold, J. High Energy Phys. 01 (2024) 144.
[27] S. Fajfer, J. F. Kamenik, I. Nisandzic, and J. Zupan, Phys. Rev. Lett. **109**, 161801 (2012).
[28] Y. Sakaki, M. Tanaka, A. Tayduganov, and R. Watanabe, Phys. Rev. D **88**, 094012 (2013).
[29] L. Calibbi, A. Crivellin, and T. Ota, Phys. Rev. Lett. **115**, 181801 (2015).
[30] S. Sahoo and R. Mohanta, Phys. Rev. D **93**, 034018 (2016).
[31] M. Bauer and M. Neubert, Phys. Rev. Lett. **116**, 141802 (2016).
[32] C. H. Chen, T. Nomura, and H. Okada, Phys. Lett. B **774**, 456 (2017).
[33] A. Crivellin, D. Müller, and T. Ota, J. High Energy Phys. 09 (2017) 040.
[34] D. Buttazzo, A. Greljo, G. Isidori, and D. Marzocca, J. High Energy Phys. 11 (2017) 044.
[35] V. Gherardi, D. Marzocca, and E. Venturini, J. High Energy Phys. 07 (2020) 225; 01 (2021) 6.
[36] V. Gherardi, D. Marzocca, and E. Venturini, J. High Energy Phys. 01 (2021) 138.
[37] A. Crivellin, D. Müller, and F. Saturnino, J. High Energy Phys. 06 (2020) 020.
[38] J. Davighi, M. Kirk, and M. Nardecchia, J. High Energy Phys. 12 (2020) 111.
[39] A. Greljo, P. Stangl, and A. E. Thomsen, Phys. Lett. B **820**, 136554 (2021).
[40] A. Carvunis, A. Crivellin, D. Guadagnoli, and S. Gangal, Phys. Rev. D **105**, L031701 (2022).
[41] J. Davighi, A. Greljo, and A. E. Thomsen, Phys. Lett. B **833**, 137310 (2022).
[42] J. Heeck and A. Thapa, Eur. Phys. J. C **82**, 480 (2022).
[43] R. L. Workman *et al.* (Particle Data Group), Prog. Theor. Exp. Phys. **2022**, 083C01 (2022).
[44] Y. S. Amhis *et al.* (Heavy Flavor Averaging Group and HFLAV Collaboration), Phys. Rev. D **107**, 052008 (2023).
[45] R. Aaij *et al.* (LHCb Collaboration), Phys. Rev. D **108**, 032002 (2023).
[46] A. J. Buras, Eur. Phys. J. C **83**, 66 (2023).
[47] J. A. Bailey *et al.* (MILC Collaboration), Phys. Rev. D **92**, 034506 (2015).
[48] H. Na *et al.* (HPQCD Collaboration), Phys. Rev. D **92**, 054510 (2015); **93**, 119906(E) (2016).
[49] D. Bigi and P. Gambino, Phys. Rev. D **94**, 094008 (2016).
[50] F. U. Bernlochner, Z. Ligeti, M. Papucci, and D. J. Robinson, Phys. Rev. D **95**, 115008 (2017); **97**, 059902(E) (2018).
[51] S. Jaiswal, S. Nandi, and S. K. Patra, J. High Energy Phys. 12 (2017) 060.
[52] P. Gambino, M. Jung, and S. Schacht, Phys. Lett. B **795**, 386 (2019).
[53] J. P. Lees *et al.* (*BABAR* Collaboration), Phys. Rev. Lett. **123**, 091801 (2019).
[54] M. Bordone, M. Jung, and D. van Dyk, Eur. Phys. J. C **80**, 74 (2020).
[55] G. Martinelli, S. Simula, and L. Vittorio, Phys. Rev. D **105**, 034503 (2022).
[56] X. G. He, G. C. Joshi, H. Lew, and R. R. Volkas, Phys. Rev. D **44**, 2118 (1991).
[57] J. Heeck and W. Rodejohann, Phys. Rev. D **84**, 075007 (2011).
[58] C. H. Chen and T. Nomura, Phys. Rev. D **96**, 095023 (2017).
[59] W. Altmannshofer, S. Gori, M. Pospelov, and I. Yavin, Phys. Rev. D **89**, 095033 (2014).
[60] W. Altmannshofer, S. Gori, M. Pospelov, and I. Yavin, Phys. Rev. Lett. **113**, 091801 (2014).
[61] W. Altmannshofer, M. Carena, and A. Crivellin, Phys. Rev. D **94**, 095026 (2016).
[62] C. H. Chen, C. W. Chiang, and C. W. Su, arXiv:2305.09256.
[63] I. Doršner, S. Fajfer, A. Greljo, J. F. Kamenik, and N. Košnik, Phys. Rep. **641**, 1 (2016).
[64] A. Biswas, S. Choubey, and S. Khan, J. High Energy Phys. 02 (2017) 123.
[65] S. N. Gninenko and N. V. Krasnikov, Phys. Lett. B **783**, 24 (2018).
[66] A. Kamada, K. Kaneta, K. Yanagi, and H. B. Yu, J. High Energy Phys. 06 (2018) 117.
[67] D. W. P. d. Amaral, D. G. Cerdeno, P. Foldenauer, and E. Reid, J. High Energy Phys. 12 (2020) 155.
[68] T. Hapitas, D. Tuckler, and Y. Zhang, Phys. Rev. D **105**, 016014 (2022).

[69] A. Bharucha, D. M. Straub, and R. Zwicky, J. High Energy Phys. 08 (2016) 098.
[70] N. Gubernari, A. Kokulu, and D. van Dyk, J. High Energy Phys. 01 (2019) 150.
[71] D. Leljak, B. Melić, and D. van Dyk, J. High Energy Phys. 07 (2021) 036.
[72] F. Mescia and C. Smith, Phys. Rev. D **76**, 034017 (2007).
[73] A. J. Buras, D. Buttazzo, J. Girrbach-Noe, and R. Knegjens, J. High Energy Phys. 11 (2015) 033.
[74] G. Isidori, F. Mescia, and C. Smith, Nucl. Phys. **B718**, 319 (2005).
[75] A. V. Artamonov *et al.* (E949 Collaboration), Phys. Rev. Lett. **101**, 191802 (2008).
[76] E. Cortina Gil *et al.* (NA62 Collaboration), J. High Energy Phys. 06 (2021) 093.
[77] Koji Shiomi, on behalf of KOTO Collaboration, *Talk Presented at KEK IPNS and J-PARC Joint Seminar* (KEK, Tsukuba, Japan, 2023).
[78] M. Fabbrichesi, E. Gabrielli, and G. Lanfranchi, *The Physics of the Dark Photon* (Springer, Cham, 2021).
[79] J. A. Bailey, A. Bazavov, C. Bernard, C. M. Bouchard, C. DeTar, D. Du, A. X. El-Khadra, J. Foley, E. D. Freeland, E. Gámiz *et al.*, Phys. Rev. D **93**, 025026 (2016).
[80] I. Doršner, S. Fajfer, N. Košnik, and I. Nišandžić, J. High Energy Phys. 11 (2013) 084.
[81] S. Iguro, T. Kitahara, Y. Omura, R. Watanabe, and K. Yamamoto, J. High Energy Phys. 02 (2019) 194.
[82] S. Hirose *et al.* (Belle Collaboration), Phys. Rev. D **97**, 012004 (2018).
[83] A. Abdesselam *et al.* (Belle Collaboration), arXiv:1903.03102.
[84] R. Aaij *et al.* (LHCb Collaboration), arXiv:2311.05224.
[85] A. G. Akeroyd and C. H. Chen, Phys. Rev. D **96**, 075011 (2017).
[86] A. Lenz, U. Nierste, J. Charles, S. Descotes-Genon, A. Jantsch, C. Kaufhold, H. Lacker, S. Monteil, V. Niess, and S. T'Jampens, Phys. Rev. D **83**, 036004 (2011).
[87] A. M. Sirunyan *et al.* (CMS Collaboration), Phys. Lett. B **819**, 136446 (2021).
[88] G. Aad *et al.* (ATLAS Collaboration), J. High Energy Phys. 06 (2021) 179.
[89] G. Aad *et al.* (ATLAS Collaboration), Phys. Rev. Lett. **125**, 051801 (2020).
[90] A. Angelescu, D. Bečirević, D. A. Faroughy, F. Jaffredo, and O. Sumensari, Phys. Rev. D **104**, 055017 (2021).
[91] L. Allwicher, D. A. Faroughy, F. Jaffredo, O. Sumensari, and F. Wilsch, J. High Energy Phys. 03 (2023) 064.
[92] L. Allwicher, D. A. Faroughy, F. Jaffredo, O. Sumensari, and F. Wilsch, Comput. Phys. Commun. **289**, 108749 (2023).